LETTER TO THE EDITOR

Positron-induced proton desorption from Ni surfaces

Y Terashima[1,6,7]**, R Arai**[1]**, T Wada**[1]**, I Kanazawa**[1]**, Y Ito**[2]**, K Fukutani**[3]**, Y Murata**[4] **and F Komori**[5]

[1] Department of Physics, Tokyo Gakugei University, Koganei, Tokyo 184-8501, Japan
[2] Research Centre for Nuclear Science and Technology, University of Tokyo, Ibaraki 319-11, Japan
[3] Institute of Industrial Science, University of Tokyo, Meguro-ku, Tokyo 153-8505, Japan
[4] The University of Electro-Communications, Chofu, Tokyo 182-8585, Japan
[5] Institute for Solid State Physics, University of Tokyo, Kashiwanoha, Kashiwa-shi, Chiba 277-8581, Japan

E-mail: terashima@bms.sanken.osaka-u.ac.jp

Abstract
Positron-induced ion-desorption spectroscopy has been constructed and used for measurements of positron-induced hydrogen ion desorption from Ni surfaces. The cross-section for proton desorption at a positron incident energy of 1.9 keV was larger than that at a positron incident energy of 2.9 keV. This value is larger than that for electron-stimulated desorption with similar incident energies, suggesting that ion desorption is caused by the thermalized positrons in the bulk.

1. Introduction

Ion desorption induced by electronic transition has been used for the study of dynamical phenomena on the surface [1]. An important motive force for this study is understanding of the dynamics of atoms and molecules on surfaces. Ishii and Murata [2, 3] have theoretically shown that the estimated cross-section for positronium formation from the adatom orbital is quite large in comparison with that of photo-excitation. Laser-induced ion desorption is considered to be useful for fundamental studies of the dynamical behaviour of adsobates [4]. However, this creates many complex excited states, and the small cross-section for ion desorption has been a disadvantage [5]. Thus we cannot obtain precise spectroscopic data using various photon energies. Positron-induced ion desorption is considered to be effectively caused by the ionization of an adatom where the bonding electron is removed by the incident low-energy

---

[6] Author to whom any correspondence should be addressed.
[7] Present address: Department of Beam Materials Science, The Institute of Scientific and Industrial Research (ISIR), Osaka University, 8-1 Mihogaoka, Ibaraki, Osaka 567-0047, Japan.

positron beam to form positronium. In addition, the recent studies with positron-annihilation-induced Auger electron spectroscopy (PAES) [6] and reflection high-energy positron diffraction (RHEPD) [7, 8] demonstrate that the low-energy positron is a strongly sensitive probe for detecting adsorbed atoms on the surface. Thus, positron-induced ion-desorption spectroscopy will provide important information on the desorption mechanism. We use low-energy positrons which are slow enough to diffuse back to a surface and reemit. The dynamical property of adsorbed atoms on a solid surface can be studied by spectroscopic analysis of desorbed ion energy.

The dynamical property of adsorbed light atoms on a solid surface is one of the most important subjects in surface science. Particularly the interaction of hydrogen with solid surfaces is of wide scientific and technological interest. The surface contamination by hydrogen atoms strongly affects the epitaxial growth of crystals, and hydrogen adsorption sometimes results in reconstruction of metal surfaces. It is still difficult to determine the local structure and dynamical properties of light atoms adsorbed on a surface. Diffuse LEED [9, 10] can be applied to this subject. However, we could not distinguish the signal of a particular adatom from that of other adsorbates.

In this letter, we explain the positron-induced ion-desorption apparatus, and then show experimental results of positron-induced proton desorption from the Ni surface. On some transition metal surfaces, it is well known that the hydrogen molecule dissociates. In positron-induced ion desorption, we pay attention to adsorbed hydrogen on a Ni surface. It is dissociatively adsorbed on this surface.

2. Method of positron-induced ion-desorption spectroscopy

The slow-positron beam for positron-induced ion-desorption spectroscopy is composed of two stages [11, 12]. The first stage of the positron beam system consists of a ^{22}Na positron source (∼3 mCi) and a W(100) foil of 1 μm thickness, which has been annealed once in a UHV chamber at ∼2000 °C and is attached near the source for moderating positrons. The intensity of the positron beam is ∼0.6 × 10^4 cps. The slow positrons are extracted from the moderator using an accelerating grid of 15 V, and are guided along the magnetic field through the solenoid tube of the first stage.

The magnetic field (60–80 Gauss) is supplied from solenoid coils directly around the vacuum transport tube, which are supplemented with Helmholtz coils at several positions where feed-through ports are present. For the positron-induced ion-desorption experiments, we need to transfer the beam from the magnetic field transport system to a magnetic-field-free region in the second stage. In the magnetic field, the radial momentum of the positron beam is converted to cyclotron motion, making it possible to collect and transport as many slow positrons as possible. At the end of the transport tube where the solenoid coil is terminated, the radius of the cyclotron motion becomes larger as the magnetic lines of force expand.

Extraction of the beam without changing the beam size is possible at the expense of increased momentum spread in the phase space. Beam extraction was accomplished by using an accelerator assembly in the magnetic field. We set the electrostatic lenses in front of the experimental chamber. The simulation of the trajectories of positrons has been performed previously [13]. This system enables us to extract positrons from a magnetic field into an electrostatic one [13–16]. We obtain electrostatic positron beams at incident energies from 2 to 4 keV at the centre of a UHV chamber, where the sample will be placed.

Figure 1 shows a schematic diagram (*a*) and a photograph of the target optics geometry in positron-induced ion-desorption spectroscopy (*b*). The mesh of the ground level is installed in front of the sample with the face of the mesh and the surface of the sample set toward
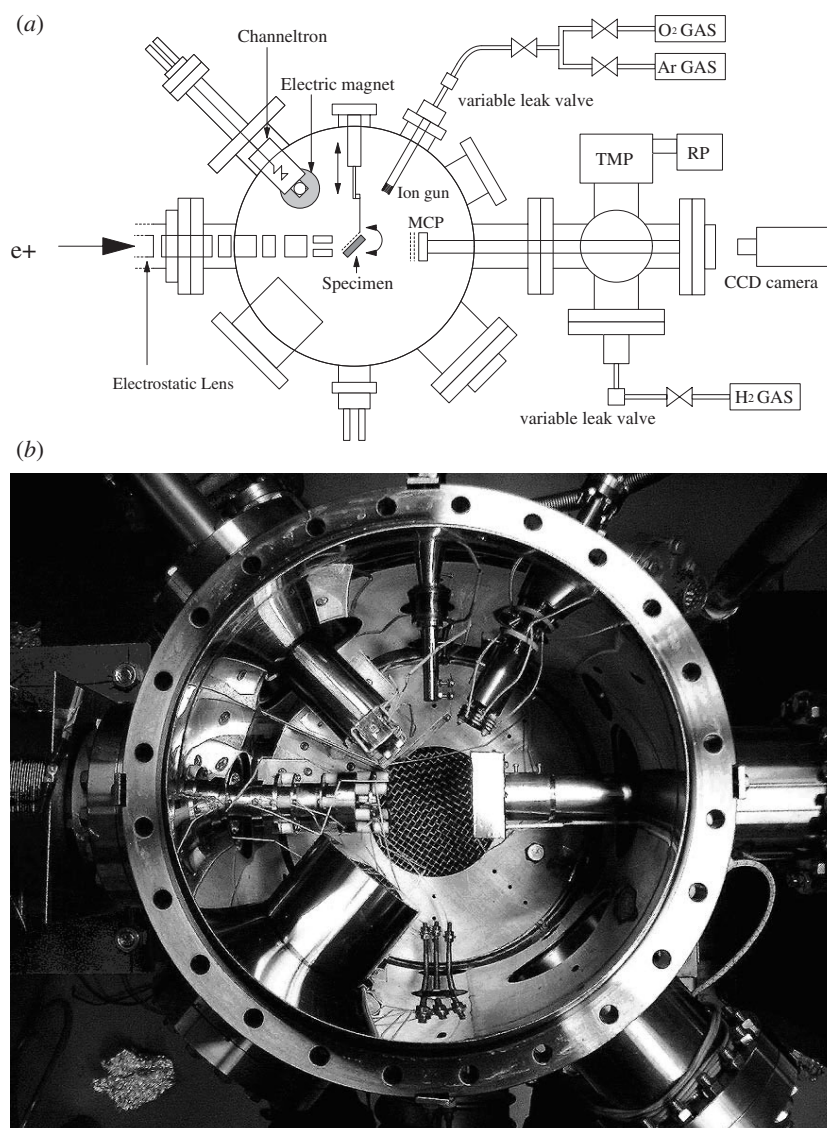
(a)

(b)

Figure 1. A schematic diagram (*a*) and a photograph (*b*) of the target optics geometry in positron-induced ion-desorption spectroscopy.

the channeltron. When 100 V is imposed on the sample, positive particles at the surface are accelerated in the direction of the channeltron. When -20 V is imposed on the sample, reflected positrons and relatively highly energetic hydrogen ions (above $\sim$20 eV) are detected by the channeltron. We can detect only desorbed ions by a magnetic field of about 25 G with the small coils in front of the channeltron, because the contamination of reemitted and reflected positrons in the signals of the desorbed positive ion is eliminated by imposing a weak magnetic field. In the case of a magnet-coil current of 5 A, the shifts of the trajectory of positron and proton beams in the kinetic energy 100 eV are $\sim$8 mm and $<$0.5 mm, respectively, as shown in figure 2. The permalloy sheet is installed between the magnet and the electrostatic lenses
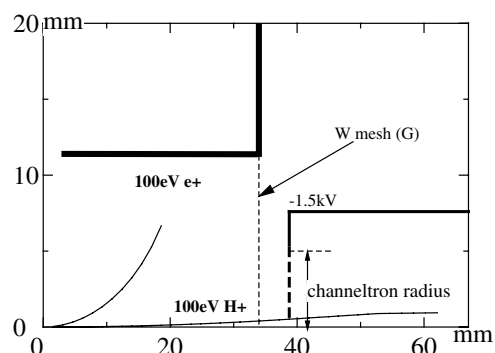
Figure 2. The shifts of trajectory of the positron and hydrogen ion beam in the case of a coil current of 5 A.

so that the magnetic field does not disturb the incident positron beam.

We must maintain the vacuum condition of 10^{-10} Torr in the experimental chamber while the chamber of the ^{22}Na source cannot be baked to establish UHV. Thus, we set an Al cylindrical block between the end of the solenoid coil and accelerator tube, whose inner diameter is 10 mm and length is 40 mm. The slow positrons are transported through the hole and are injected into the UHV experimental chamber. When the valve between the positron beam and the sample chamber is opened, the pressure of the UHV chamber increases to 2.0×10^{-10} from 8.2×10^{-11} Torr.

The sample is suspended by W wires and can be annealed by direct current through the wires. The highly pure hydrogen, oxygen and argon gas holders are connected with the UHV chamber. The specimen surface was cleaned by repeated argon ion bombardment and annealing to 1000 K. Finally, the clean Ni surface was annealed for 30 min at ~1000 K to eliminate defects in 2.0×10^{-10} Torr. Then, hydrogen gas at 1.0×10^{-8} Torr was introduced in the sample chamber for 5 min through a liquid nitrogen trap to adsorb hydrogen on the clean Ni surface [17].

3. Hydrogen ion desorption from a Ni surface

The energy gain from the coupling between H 1s and Ni 3d electrons results in a hydrogen bonding level, and explains the chemisorption energy for H on the Ni surface [18]. Hybridization of the H 1s with the d band makes an antibonding level above the d band. In the Ni surface, this antibonding state is near the Fermi level, and will not weaken the hydrogen–metal bond. When the slow positron picks up an electron in the H–Ni bonding state to form positronium, we can recognize it as the ionization of the adsorbate. We use a simple assumption that the cross-section for the ion desorption is proportional to that of the ionization [19],

$$\delta_d = A\delta_i, \tag{1}$$

where δ_d and δ_i are the cross-section for the ion desorption and ionization due to positronium formation, respectively. A is a function of the initial and final states of the ionization. The reneutralization contribution is therefore considered to be included in the factor A.

The matrix element of positronium formation is shown as follows [2]:

$$M_{if} = \int \psi^*(r_+, r_-) V(r_+, r_-) \phi_+(r_+) \phi_-(r_-) \, dr_+ \, dr_-, \tag{2}$$
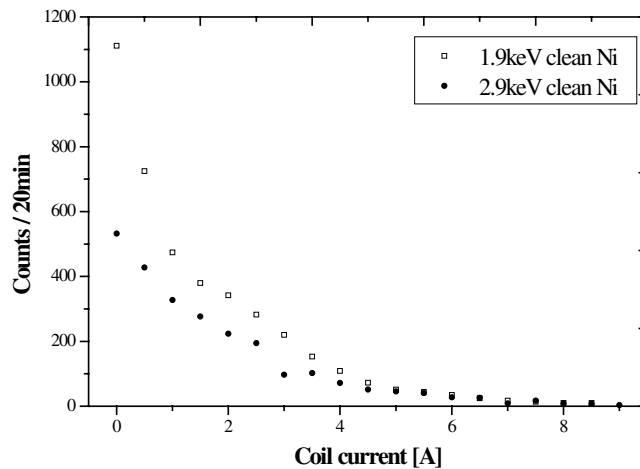
Figure 3. Counts of positive particles versus the coil current, from a clean Ni surface.

where $\psi^*(r_+, r_-)$ is the positronium (Ps) wavefunction at the surface. An electron wavefunction in a bonding state of the H adsorbed on the Ni surface and a reemitted slow positron wavefunction are represented as $\phi_-(r_-)$ and $\phi_+(r_+)$, respectively. The interaction $V(r_+, r_-)$ is the screened Coulomb interaction. Taking $\alpha = a_0^{-1} + \mu$ (a_0 is the Ps radius and μ is a screening parameter), we can represent this as

$$V(r_+, r_-) = \frac{\exp(-\alpha|r_+ - r_-|)}{|r_+ - r_-|}. \tag{3}$$

Figure 3 plots the number of positive particles emitted from the clean Ni surface versus the coil current, which is proportional to the magnetic field in front of the channeltron. In these experiments, the incident energies of positrons are 1.9 and 2.9 keV. The count with the coil current of 0 A includes both reemitted positrons and desorbed ions. As the coil current increases, reemitted positrons are eliminated. Therefore we conclude that the count with the coil current of $\sim$5 A indicates desorbed ions. When there is no positron incidence, the value of background is $<$0.7 counts/20 min. The number of desorbed ions from the clean Ni surface at the incident energies of 1.9 and 2.9 keV is $<$0.5 counts min^{-1} at a coil current of 7–9 A as we can see in figure 3. This result means that desorbed ions are hardly detected at these currents. The number of positrons reemitted at the incident energy of 1.9 keV is larger than that at the incident energy of 2.9 keV.

We can understand this result by considering the positron implantation profiles in the Ni at the incident energies of 1.9 and 2.9 keV. The positrons of incident energy 2.9 keV are injected to the bulk more deeply than positrons of incident energy 1.9 keV. The number of thermalized positrons which return to the surface increases as the positron incident energy decreases.

Figure 4 plots the relation between the number of positive particles (positrons and ions) emitted from the H-saturated Ni surface and the coil current, which is proportional to the magnetic field in front of the channeltron. We can interpret that the number of desorbed ions at coil currents of higher than 6 A corresponds to hydrogen ions. The number of desorbed hydrogen ions at an incident energy of 1.9 keV is larger than that at 2.9 keV.

When -20 V is imposed on the sample, a few positive particles are emitted, which correspond to reflected positrons and relatively highly energetic hydrogen ions ($\sim$20 eV).
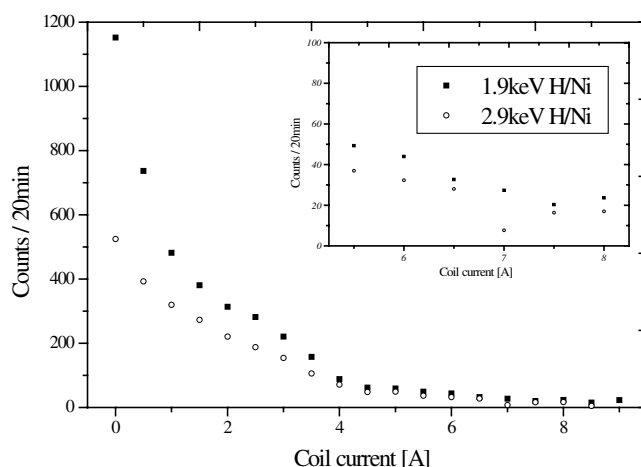
Figure 4. Counts of positive particles (positrons and hydrogen ions) versus the coil current from a H-adsorbed Ni surface.

Eliminating this effect, we can experimentally determine the cross-section, as follows:

$$\frac{C_i}{C_p} = NA|M|^2 \qquad (4)$$

where M is shown in equation (2), A is the factor in equation (1), N is the hydrogen number per surface unit cell, C_i is the number of desorbed ions, which is obtained by subtracting the number of desorbed ions at 2.9 keV from that at 1.9 keV at coil currents of 6–8 A, and C_p is the number of thermalized positrons. The number of emitted positrons is obtained by subtracting the number of positrons reemitted at 2.9 keV from that at 1.9 keV at coil currents of 0 A. When it is assumed that emitted slow positrons, emitted positronium and slow positrons trapped to the surface state are branched approximately in the same fraction, we can experimentally estimate the effective cross-section, $A|M|^2$, to be 2.8×10^{-18} cm^2. This effective cross-section is three orders of magnitude higher than that of the electron-stimulated desorption [20].

About half of the incident positrons can return with thermal energy from the bulk to the surface, and stay in the surface state for several hundred picoseconds. Thus the surface-state positrons can introduce the observed large cross-section for positron-induced hydrogen ion desorption. That is, the desorption is mainly initiated by the positronium formation between the surface-state positrons and the bonding electrons of the adsorbed hydrogens.

4. Conclusion

We have constructed positron-induced ion-desorption spectroscopy with an electrostatic positron beam. We have performed the measurements of positron-induced proton desorption from the Ni surfaces, and have estimated the effective cross-section of the positron-induced proton desorption on the H/Ni surface.

References

[1] Lin M C and Ertl G 1986 *Annu. Rev. Phys. Chem.* **37** 287
[2] Ishii A and Murata Y 1992 *Surf. Sci.* **273** 442
[3] Ishii A and Murata Y 1992 *Mater. Sci. Forum* **105–110** 297
[4] Fukutani K and Murata Y 1997 *Surf. Sci.* **390** 164
[5] Mase M, Mizuno S, Yamada M, Doi I, Katsumi T, Watanabe S, Achiba Y and Murata Y 1989 *J. Chem. Phys.* **91** 590
[6] Weiss A, Mayer R, Jibaly M, Lei C, Mehl D and Lynn K G 1988 *Phys. Rev. Lett.* **61** 2245
[7] Kanazawa I *et al* 1995 *Appl. Surf. Sci.* **85** 124
[8] Kawasuso A and Okada S 1998 *Phys. Rev. Lett.* **81** 2695
[9] Pendry J B and Saldin D K 1984 *Surf. Sci.* **145** 33
[10] Heintz K, Saldin D K and Pendry J B 1985 *Phys. Rev. Lett.* **55** 2312
[11] Kanazawa I, Nakajyo T, Tashiro M, Komori F, Murata Y, Fukutani K and Ito Y 1997 *Appl. Surf. Sci.* **116** 129
[12] Kanazawa I, Koizumi T, Iwamoto A, Tashiro M, Komori F, Murata Y, Fukutani K and Ito Y 1997 *Mater. Sci. Forum* **255–257** 787
[13] Kanazawa I, Nakajyo T, Tashiro M, Komori F, Murata Y, Fukutani K and Ito Y 1997 *Appl. Surf. Sci.* **116** 129
[14] Sueoka O, Yamazaki M and Ito Y 1989 *J. Appl. Phys.* **28** L166
[15] Ito Y, Yamazaki M, Sueoka O, Kanazawa I, Mashiko K, Ichimiya A, Murata Y, Okada S, Hasegawa M and Hyodo T 1991 *Nucl. Instrum. Methods* A **305** 269
[16] Kanazawa I, Iwamoto A, Ozaki A, Terashima Y, Ito Y, Fukutani K, Murata Y and Komori F 1999 *Appl. Surf. Sci.* **149** 248
[17] Chiristmann K, Behm R J, Ertl G, Hove M A V and Weinberg W H 1979 *J. Chem. Phys.* **70** 4168
[18] Hammer B and Scheffler M 1995 *Phys. Rev. Lett.* **74** 3487
[19] Ishii A and Pendry J B 1989 *Surf. Sci.* **209** 23
[20] Takano A and Ueda K 1993 *Japan. J. Appl. Phys.* **32** 1217